AIP Applied Physics Letters

Recombination dynamics of a localized exciton bound at basal stacking faults within the m-plane ZnO film

S. Yang, H. C. Hsu, W.-R. Liu, B. H. Lin, C. C. Kuo, C.-H. Hsu, M. O. Eriksson, P. O. Holtz, and W. F. Hsieh

Citation: Applied Physics Letters **105**, 011106 (2014); doi: 10.1063/1.4887280
View online: http://dx.doi.org/10.1063/1.4887280
View Table of Contents: http://scitation.aip.org/content/aip/journal/apl/105/1?ver=pdfcov
Published by the AIP Publishing

Articles you may be interested in
Surface related and intrinsic exciton recombination dynamics in ZnO nanoparticles synthesized by a sol-gel method
Appl. Phys. Lett. **102**, 013109 (2013); 10.1063/1.4774002

Photoluminescence associated with basal stacking faults in c-plane ZnO epitaxial film grown by atomic layer deposition
Appl. Phys. Lett. **100**, 101907 (2012); 10.1063/1.3692730

Exciton localization on basal stacking faults in a -plane epitaxial lateral overgrown GaN grown by hydride vapor phase epitaxy
J. Appl. Phys. **105**, 043102 (2009); 10.1063/1.3075596

Complex excitonic recombination kinetics in ZnO: Capture, relaxation, and recombination from steady state
Appl. Phys. Lett. **90**, 041917 (2007); 10.1063/1.2432259

Radiative recombination centers induced by stacking-fault pairs in ZnSe/ZnMgSSe quantum-well structures
Appl. Phys. Lett. **75**, 3944 (1999); 10.1063/1.125502

This article is copyrighted as indicated in the article. Reuse of AIP content is subject to the terms at: http://scitation.aip.org/termsconditions. Downloaded to IP: 140.113.38.11 On: Thu, 25 Dec 2014 02:22:50

Recombination dynamics of a localized exciton bound at basal stacking faults within the *m*-plane ZnO film

S. Yang,[1] H. C. Hsu,[2,a)] W.-R. Liu,[1] B. H. Lin,[1,3] C. C. Kuo,[3] C.-H. Hsu,[1,3] M. O. Eriksson,[4] P. O. Holtz,[4] and W. F. Hsieh[3,a)]
[1]*Scientific Research Division, National Synchrotron Radiation Research Center, Hsinchu 30076, Taiwan*
[2]*Department of Photonics and Advanced Optoelectronic Technology Center, National Cheng Kung University, 701 Tainan, Taiwan*
[3]*Department of Photonics and Institute of Electro-Optical Engineering, National Chiao Tung University, Hsinchu 30010, Taiwan*
[4]*Department of Physics, Chemistry and Biology (IFM), Linköping University, Linköping, Sweden*

(Received 12 March 2014; accepted 24 June 2014; published online 7 July 2014)

We investigated the carrier dynamics near basal stacking faults (BSFs) in *m*-plane ZnO epitaxial film. The behaviors of the type-II quantum wells related to the BSFs are verified through time-resolved and time-integrated photoluminescence. The decay time of the emission of BSFs is observed to have a higher power law value and longer decay time than the emission of the donor-bound excitons. The spectral-dependent decay times reveal a phenomenon of carriers migrating among band tail states, which are related to the spatial distribution of the type-II quantum wells formed by the BSFs. A high density of excited carriers leads to a band bending effect, which in turn causes a blue-shift of the emission peak of BSFs with a broadened distribution of band tail states. © *2014 AIP Publishing LLC*. [http://dx.doi.org/10.1063/1.4887280]

ZnO, a wide direct band gap material, has attracted much attention due to its potential for applications in ultraviolet photonic devices.[1–4] The presence of the built-in electric field in *c*-plane-grown ZnO reduces the emission efficiency. To avoid this problem, much research has been focused on the growth of non-polar (*a*- or *m*-planes) ZnO epitaxial films. Since ZnO substrates are very rare and expensive, other foreign substrates, such as sapphire, SiC, and $LaAlO_3$, are the most commonly used substrates to grow nonpolar ZnO and related alloys. Therefore, this heteroepitaxy results in the generation of a high density of structural defects, such as dislocations and stacking faults. The heteroepitaxial non-polar epitaxial films suffer from a high density of basal stacking faults (BSFs). From the viewpoint of crystal growth, defects such as BSFs should be eliminated or at least significantly reduced. Several growth methods have been proposed to reduce the density of BSFs in ZnO and III-Nitride materials.[5] In contrast, some of these defects have exposed unusual properties, which have potential to be employed in particular applications. Interestingly, BSFs exhibiting optical activity strongly influence the luminescence properties of the materials with wurtzite structure such as GaN and ZnO.[6–10] Through *ab initio* calculations, the BSF is predicted to have the zinc-blend (ZB) lattice structure embedded in the wurtzite (WZ) ZnO matrix, which forms a type-II quantum well (QW).[11] Besides possible applications as lighting devices, the type-II QW structures in semiconductor materials are promising for photovoltaic devices as a result of their spatial separation of photoexcited electrons and holes.[12,13] Consequently, this ZnO-based spontaneously formed type-II QW system has become alternatively important. Although it is essential to understand the luminescence mechanism and to investigate the photoexcited carrier dynamics, published reports on the experimental aspects of the carrier dynamic properties of this material system have been limited up to now. In this article, we present a detailed emission mechanism of the BSFs in the *m*-plane ZnO layers. We report on some peculiar behaviors such as S-shaped peak shifting due to the composition fluctuation and the migration of photoexcited carriers among the band tail states. The high density of electrons accumulated at the interface between the potential well and barrier result in a band bending effect that broadens the distribution of these energy levels and decreases the decay times.

An epitaxial *m*-plane ZnO layer with a thickness of 130 nm was grown on *m*-plane sapphire substrates by the atomic layer deposition (ALD) method (for details, see Ref. 14). The TEM results show that BSFs are the predominant defect with a density of $\sim 10^6\,cm^{-1}$. For the transient photoluminescence (PL) measurements, the excitation from the third harmonic ($\lambda_{exc} = 266$ nm) of a Ti:sapphire femtosecond pulsed laser (pulse width 150 fs) with the repetition rate of 76 MHz was employed, and the laser spot was focused down to about 1 μm. The time-resolved PL (TR-PL) signal was detected by a UV-sensitive Hamamatsu streak camera with a temporal resolution better than 20 ps.

The low-temperature time-integrated PL (TI-PL) spectra of the sample with different excitation powers are shown in Figure 1(a). The dominating emission at 3.32 eV results from the BSFs, and the emission centered at 3.37 eV is attributed to the near-band-edge (NBE) emission bands consisting of the donor-bound exciton (D^0X) and the free exciton (FX).[7] The D^oX emission has a rather broad width (FWHM ~ 22 meV) as compared with those of the pulsed-laser-deposition-grown ZnO films (FWHM ~ 10 meV and typical 9–15 meV).[15,16] Some of the literature[17–19] has reported that D^oX emissions with a lifetime range from 230 to 370 ps were observed in

a)Authors to whom correspondence should be addressed. Electronic addresses: hsuhc@mail.ncku.edu.tw and wfhsieh@mail.nctu.edu.tw

 © 2014 AIP Publishing LLC

This article is copyrighted as indicated in the article. Reuse of AIP content is subject to the terms at: http://scitation.aip.org/termsconditions. Downloaded to IP: 140.113.38.11 On: Thu, 25 Dec 2014 02:22:50

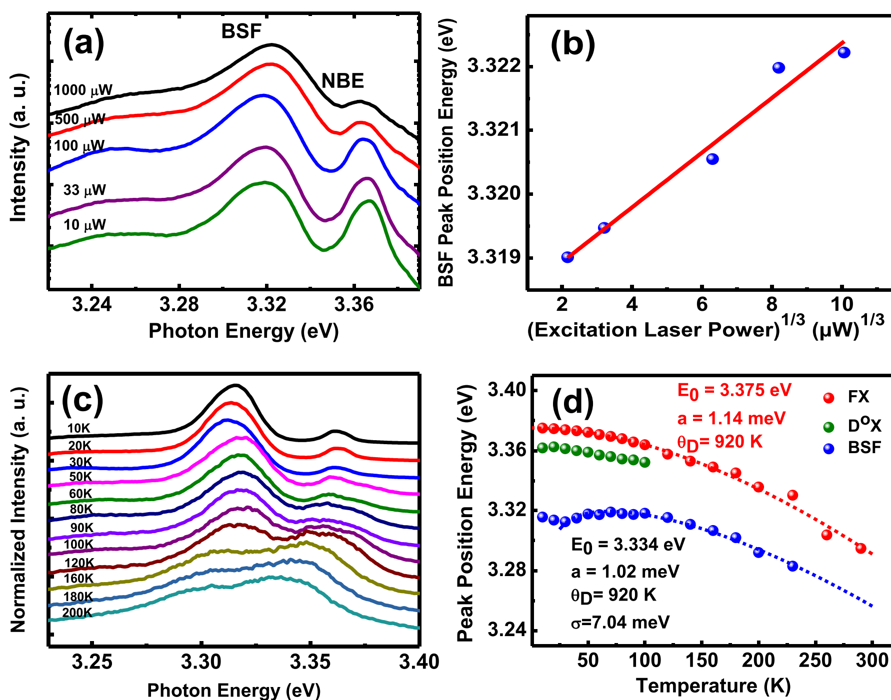

FIG. 1. (a) Power dependent TI-PL spectra recorded at 5 K of the ZnO film grown by ALD and annealed at 600 °C. (b) The intensity versus the excitation power of the BSF and NBE emissions. The dashed lines represent the outcome of the power-law fitting work. (c) The temperature dependent TI-PL spectra of the ZnO film taken between 10 and 200 K. (d) The energy versus temperature plot of the BSF and NBE emissions. The dashed lines depict the fitting results to the Varshni's law.

high-quality ZnO thin film, with a line width of less than 5 meV. Compared to these reported results, the rather large line width and short lifetime of the D^oX emission in this paper could be due, we believe, to defects such as Zinc vacancy and/or BSFs, which may have enhanced the non-radiative transition from the D^oX. The energy peak of the BSF emission reveals a blueshift from 3.319 to 3.322 eV as the excitation power is increased, and the peak energy as a function of the excitation power is shown in Figure 1(b). In type-II heterostructures of other material systems, a blueshift of the peak energy due to excitation power increment has been reported.[20,21] In our case, the electrons and holes are spatially separated in different regions; that is, the electrons are confined in the ZB structure of the ZnO layer, and the holes are localized in the WZ structure of the ZnO layer. The well width formed by BSFs is 0.8 nm (exactly 1.5 times that of the c-axis lattice constant)[9] less than the exciton Bohr radius of 2.3 nm, which leads to the zero Stokes-shift that originated from the screening effect.[22,23] Therefore, the blueshift for increasing excitation power may not be a result of screening the electric fields. Such spatial separation between electrons and holes leads to an electric field, which gives rise to the bending of the valence and conduction band. The electrons and holes accumulated at the interface result in the formation of the potential well, which can be treated as approximately triangular. Thus, the electron quantization energy is expected to be proportional to the third root of the excitation power.[24] As shown in Figure 1(b), the PL peak position energy can be fitted well by the third root of the excitation power, which indicates that the blueshift indeed originates from the recombination in the type-II QWs.[25,26]

In Figure 1(c), the energy peak of the BSF emission (marked by solid black circles) has a peculiar shift with raising temperature: the peak energy as a function of the temperature is shown in Figure 1(d) and termed as a "S-shape behavior," which is attributed to the localization effect observed on the excited carriers in the QWs.[27] The S-shape behavior can be explained by band filling in the tails of the density-of-states (DOS), which implies that band tail states exist in the *m*-plane ZnO thin film. The model assumes that there are a certain amount of trap states forming the band tails with the DOS of Gaussian distribution, and the temperature-dependent peak energy is given by[28]

$$h\nu_0 = E_0 - \frac{\sigma^2}{k_B T}, \tag{1}$$

where E_0 is the transition energy determined by the centers of the DOS Gaussian distributions of the electrons in the band tail and the holes in the valance band, and $\sigma^2/k_B T$ is the Stokes-type redshift, and where σ is the dispersion of the Gaussian of the band tail, which is correlated to the localization energy. The quantity E_0 relates to the band gap described by Varshni's equation; therefore, the temperature-dependent equation of the peak energy can be described as

$$E_0(T) = E_0(0) - \frac{\alpha T^2}{T+\beta} - \frac{\sigma^2}{k_B T}. \tag{2}$$

From the fitting of the S-shaped curve of the BSF peak energy as a function of the temperature to Eq. (3) (see Fig. 1(d)), the parameter values of $E_0(0) \approx 3.334$ eV, $\alpha \approx 1.02$ meV, $\beta \approx 920$ K, and $\sigma \approx 7.04$ meV are obtained. The fitting results reveal that the BSF emission at low temperatures originates from the transition between the electrons trapped in the QWs formed by the BSFs and the holes in the valance band. Then the electrons in the QWs are further trapped into the band tail states. Subsequently, the electrons in the QWs and the holes in the valance band are considered to form BSF-bound excitons, which are further confined into the band tail states. The NBE emission is composed of the D^oX (marked by hollow red circles) and the FX (solid red circles) transitions. In

This article is copyrighted as indicated in the article. Reuse of AIP content is subject to the terms at: http://scitation.aip.org/termsconditions. Downloaded to IP: 140.113.38.11 On: Thu, 25 Dec 2014 02:22:50

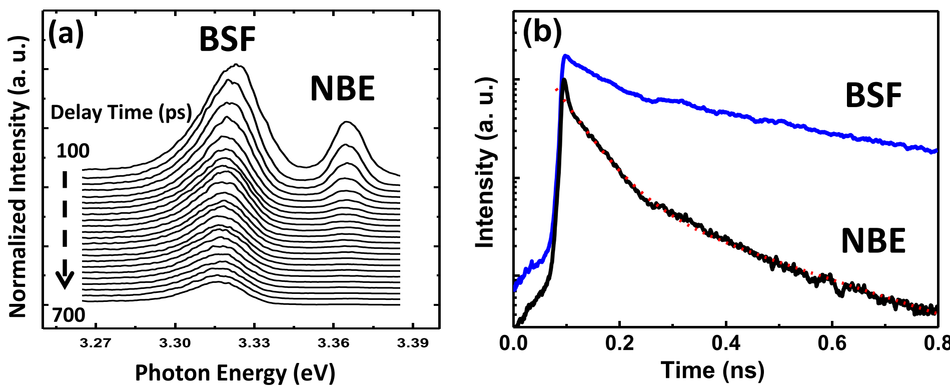

FIG. 2. (a) TR-PL spectra with time delays in steps of 100 ps after the laser pulse measured at 5 K with an excitation power of 100 μW. Each curve has the integrated time of 25 ps, and the time interval between each other is 25 ps. (b) The decay curves of the intensity integrated from the BSF and NBE emissions in energy ranges of 3.280–3.345 eV and 3.345–3.397 eV, respectively. The decay curve at the bottom is the response of the instrument.

Figure 1(d), the peak energy of the FX transition as a function of temperature is fitted to Varshni's formula, which is shown as a red dashed line and determines the transition energy at 0 K to be about 3.375 eV. The FX tends to be bound by a donor to form D^oX below 100 K, which is consistent with previous observations.[29] To confirm this assumption, we performed TR-PL measurements. In Figure 2(a), the TR-PL spectra at a temperature of 5 K are monitored after a pulsed excitation. With increasing time after the pulse, the BSF emission band shows a redshift from 3.322 to 3.315 eV, while the NBE emission band remains at about 3.362 eV. Such an observed behavior is a typical feature for a relaxation process of the BSF-bound electrons in the band tail states.[30] To determine the average decay times of the BSF and NBE emission bands, the decay curves are plotted in Figure 2(b). The decay curve of the BSF (NBE) emission band is obtained by integrating the intensity in the energy range from 3.280 to 3.345 eV (from 3.345 to 3.397 eV). Each decay curve is fitted by a bi-exponential function: $I(t) = A_1 \exp(-t/\tau_1) + A_2 \exp(-t/\tau_2)$. For the NBE emission, the decay times are determined to be $\tau_1 \approx 52$ ps, $\tau_2 \approx 250$ ps, and the ratio of A_1/A_2 is about 8.3, which means that τ_1 is the decay time of the NBE in which the D^oX transition dominates. The decay time of the NBE band agrees with the reported lifetime of D^oX, and τ_2 is the decay time resulting from the free exciton transition.[31,32] For the BSF emission, the decay times are $\tau_1 \approx 55$ ps and $\tau_2 \approx 450$ ps. Corfdir *et al.* reported the decay curves of the emissions in BSFs of the GaN a-plane films.[33] They found that bi-exponential decay curves only occur in the region of the BSFs bundles. The origin of the shorter decay time τ_1 is attributed to the complex overlapping of electron and hole wave function in the different distributions of inter-BSF distances. The longer decay time τ_2 is due to the radiative recombination of the BSF-bound electrons with the holes in the W-ZnO.[26] Using the rate equation analysis,[34] the rate equations of the transitions of FX-to-D^0X and FX-to-BSF could be written as follows:

$$dn_{DX}/dt = n_{FE}/\tau_{FE\rightarrow DX} - n_{DX}/\tau_{DX}, \tag{3}$$

$$dn_{BSF}/dt = n_{FE}/\tau_{FE\rightarrow BSF} - n_{BSF}/\tau_{BSF}, \tag{4}$$

where n_{FE} is the density of the free excitons, τ_{FE} is the lifetime of the free exciton, and the constants $\tau_{FE\rightarrow DX}$ and $\tau_{FE\rightarrow BSF}$ are the lifetimes of the capture transitions of FX-to-D^0X and FX-to-BSF, respectively. In the steady state, the dn_{DX}/dt and dn_{BSF}/dt in the rate equations are zero. Besides, the intensities of FX, D^0X, and BSF are presented as $I_{FE} = n_{FE}/\tau_{FE}$, $I_{DX} = n_{DX}/\tau_{DX}$, and $I_{BSF} = n_{BSF}/\tau_{BSF}$. Therefore, we could obtain the lifetimes of the capture transitions of FX-to-D^0X ($\tau_{FE\rightarrow DX}$) and FX-to-BSF ($\tau_{FE\rightarrow BSF}$) from Eqs. (3) and (4)

$$\tau_{FE\rightarrow DX} = I_{FE}\tau_{FE}/I_{DX}, \tag{5}$$

$$\tau_{FE\rightarrow BSF} = I_{FE}\tau_{FE}/I_{BSF}. \tag{6}$$

Based on the PL results, the intensity ratio of D^0X to FE is about 8.3 and the lifetime of the FX is $\sim$250 ps. Therefore, the value of $\tau_{FE\rightarrow DX}$ can be roughly estimated to be about 6 ps. Similarly, the intensity ratio of BSF to FX is about 1.67×10^4, so the value of $\tau_{FE\rightarrow BSF}$ can be roughly estimated to be 15 fs.

To gain more information on the details of the band tails, spectrally dependent decay times are plotted. In Figure 3, the PL decay times at different monitored emission energies are plotted together with the corresponding TI-PL spectra (solid curves). The decay times of the BSF emission gradually increase with decreasing emission energy, while the NBE emission appears to have fixed decay times of the D^oX transition for an excitation power of 100 μW in Figure 3(a). Such a significant difference implies that carriers migrating among band tail states will occur for the BSFs. In the energy range of the BSF emission band, the density of band tail states is estimated to follow $\exp(-E/E_o)$, and the radiative recombination time τ_r as a constant does not vary with altered emission energies. The decay time $\tau(E)$ can be expressed as[30,35]

$$\tau(E) = \frac{\tau_r}{1 + \exp\left[(E - E_{me})/E_o\right]}, \tag{7}$$

where E_{me} is the characteristic energy, which plays a role analogous to that of a mobility edge, and the inverse value of the radiative recombination time corresponds to the transfer rate for electrons from the band tail states to the valance band. The parameter E_o represents the characteristic energy of the density distribution of the band tail states, which also plays a role analogous to the depth of the band tail state.[31,36] Spectrally dependent decay time curves with excitation powers from 10 to 1020 μW at 5 K (not shown here) reveal an ambiguous cross at $\sim$3.33 eV. This observation implies that the value of E_{me} is consistent with 3.33 eV, evaluated from Eq. (4). For the case of an excitation laser power of 100 μW, the best fits in Figure 3(a) are $\tau_r = 758$ ps, $E_{me} = 3.33$ eV, and $E_0 = 18$ meV. As the temperature is

This article is copyrighted as indicated in the article. Reuse of AIP content is subject to the terms at: http://scitation.aip.org/termsconditions. Downloaded to IP: 140.113.38.11 On: Thu, 25 Dec 2014 02:22:50

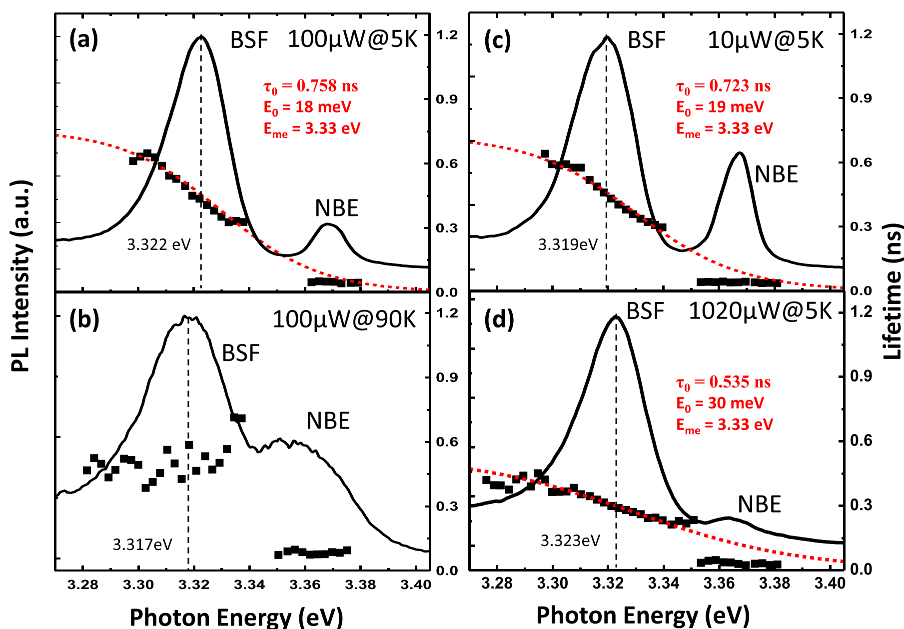

FIG. 3. The spectrally dependent decay times are plotted with the same excitation power, 100 μW, at different temperatures; (a) 5 and (b) 90 K, and with different excitation power; (c) 10 and (d) 1020 μW at the same temperature 5 K.

raised to 90 K, the curve of the decay times versus the monitored photon energy (in Fig. 3(b)) in the BSF emission band reveals an almost constant value of about 450 ps. Such result indicates that the BSF-bound excitons are delocalized from the band tail states by thermal excitation at 90 K. Further, we performed TR-PL with excitation powers of 10 μW and 1020 μW at 5 K, and the decay times versus the photon energy are shown in Figures 3(c) and 3(d). The best fitting results yield $\tau_r = 723$ ps (535 ps) and $E_o = 19$ meV (30 meV) for an excitation power of 10 μW (1020 μW). The band profile of the QWs structure grown along the polar axis should be tilted by the internal electric field that leads to QWs of triangular shape, which is in agreement with the results of power-dependent TI-PL. Therefore, a high density of excited carriers is produced by the high excitation power, and they accumulate at the interface between the potential well and barrier due to the Coulomb attraction, which results in a band bending effect that raises the electron quantization energy as mentioned above and enhances the overlap of the wave functions of the electron and the hole. Such an enhancement of the wave function overlap is in agreement with the decrease of the radiative recombination time τ_r at high excitation power in Figure 3(d). Besides, the electron quantization energy level increases, which means an increased separation between the energy levels among the band tails states followed by a broadening of the distribution. This fact raises the value of E_o, as observed in Figure 3(d). The separation between the energy levels among the band tail states is also considered to increase with high excitation laser power due to the band bending effect, which results in a high density of photon-excited carriers.

In conclusion, we have studied BSFs-related localized carrier recombination dynamics in the m-plane ZnO epitaxial films. The randomly distributed type-II QWs are formed by the high density of BSFs in the ZnO materials, leading to a wave function coupling between the BSF-bound electrons. By TI-PL and TR-PL measurements, which represent the carrier dynamics in the BSFs, reveal the migration behavior of the BSF-bound excitons in the band tails states. High excitation laser power leads to a band bending effect, which in turn broadens the distribution of the band tail states, and subsequently increases the depth of the distribution as well as causing an energy shift of the emission band due to the type-II QWs.

The authors are thankful to P. Bergman in IFM for providing the time-resolved facilities. This work was partly supported by National Science Council of Taiwan under Grant Nos. NSC-99-2112-M-006-017-MY3, NSC-100-2112-M-213-002-MY3, and NSC-102-2112-M-006-012-MY3.

[1]Ü. Özgür, Ya. I. Alivov, C. Liu, A. Teke, M. A. Reshchikov, S. Doğan, V. Avrutin, S.-J. Cho, and H. Morkoç, J. Appl. Phys. **98**, 041301 (2005).
[2]D. C. Look, D. C. Reynolds, C. W. Litton, R. L. Jones, D. B. Eason, and G. Cantwell, Appl. Phys. Lett. **81**, 1830 (2002).
[3]T. Wang, H. Wu, H. Zheng, J. B. Wang, Z. Wang, C. Chen, Y. Xu, and C. Liu, Appl. Phys. Lett. **102**, 141912 (2013).
[4]W.-R. Liu, Y.-H. Li, W. F. Hsieh, W. C. Lee, M. Hong, J. Kwo, and C.-H. Hsu, J. Phys. D: Appl. Phys. **41**, 65105 (2008).
[5]R. Ravash, P. Veit, M. Müller, G. Schmidt, A. Dempewolf, T. Hempel, J. Bläsing, F. Bertram, A. Dadgar, J. Christen, and A. Krost, Phys. Status Solidi C **9**, 507 (2012).
[6]S. Yang, C. C. Kuo, W.-R. Liu, B. H. Lin, H. C. Hsu, C. H. Hsu, and W. F. Hsieh, Appl. Phys. Lett. **100**, 101907 (2012).
[7]W. H. Lin, U. Jahn, H. T. Grahn, L. Chang, M. M. C. Chou, and J. J. Wu, Appl. Phys. Express **6**, 061101 (2013).
[8]W. Rieger, R. Dimitrov, D. Brunner, E. Rohrer, O. Ambacher, and M. Stutzmann, Phys. Rev. B. **54**, 17596 (1996).
[9]P. Corfdir, P. Lefebvre, J. Levrat, A. Dussaigne, J.-D. Ganiere, D. Martin, J. Ristic, T. Zhu, N. Grandjean, and B. Deveaud-Pledran, J. Appl. Phys. **105**, 043102 (2009).
[10]Y. J. Sun, O. Brandt, U. Jahn, T. Y. Liu, A. Trampert, S. Cronenberg, S. Dhar, and K. H. Ploog, J. Appl. Phys. **92**, 5714 (2002).
[11]Y. Yan, G. M. Dalpian, M. M. Al-Jassim, and S.-H. Wei, Phys. Rev. B. **70**, 193206 (2004).
[12]Y. Zhang, L.-W. Wang, and A. Mascarenhas, Nano Lett. **7**, 1264 (2007).
[13]J. Schrier, D. O. Demchenko, L.-W. Wang, and A. P. Alivisatos, Nano Lett. **7**, 2377 (2007).
[14]S. Yang, B. H. Lin, C. C. Kuo, H. C. Hsu, W.-R. Liu, M. O. Eriksson, P.-O. Holtz, C.-S. Chang, C.-H. Hsu, and W. F. Hsieh, Cryst. Growth Des. **12**, 4745 (2012).
[15]W.-R. Liu, W. F. Hsieh, C.-H. Hsu, K. S. Liang, and F. S.-S. Chien, J. Appl. Cryst. **40**, 924 (2007).
[16]W.-R. Liu, Y.-H. Li, W. F. Hsieh, C.-H. Hsu, W. C. Lee, Y. J. Lee, M. Hong, and J. Kwo, Cryst. Growth Des. **9**, 239 (2009).

This article is copyrighted as indicated in the article. Reuse of AIP content is subject to the terms at: http://scitation.aip.org/termsconditions. Downloaded to IP: 140.113.38.11 On: Thu, 25 Dec 2014 02:22:50

[17]M. R. Wagner, G. Callsen, J. S. Reparaz, J.-H. Schulze, R. Kirste, M. Cobet, I. A. Ostapenko, S. Rodt, C. Nenstiel, M. Kaiser, A. Hoffmann, A. V. Rodina, M. R. Phillips, S. Lautenschläger, S. Eisermann, and B. K. Meyer, Phys. Rev. B **84**, 035313 (2011).
[18]A. Zeuner, H. Alves, D. M. Hofmann, B. K. Meyer, M. Heuken, J. Biasing, and A. Krost, Appl. Phys. Lett. **80**, 2078 (2002).
[19]Y. Chen, H. J. Ko, S. K. Hong, and T. Yao, Appl. Phys. Lett **76**, 559 (2000).
[20]S.-Y. Lin, C.-C. Tseng, W.-H. Lin, S.-C. Mai, S.-Y. Wu, S.-H. Chen, and J.-I. Chyi, Appl. Phys. Lett. **96**, 123503 (2010).
[21]T. Kawazu, T. Mano, T. Noda, and H. Sakaki, Appl. Phys. Lett. **94**, 081911 (2009).
[22]T. Kuroda and A. Tackeuchi, J. Appl. Phys. **92**, 3071 (2002).
[23]S. F. Chichibu, A. C. Abare, M. P. Mack, M. S. Minsky, T. Deguchi, D. Cohen, P. Kozodoy, S. B. Fleischer, S. Keller, J. S. Speck, J. E. Bowers, E. Hu, U. K. Mishra, L. A. Coldren, S. P. DenBaars, K. Wada, T. Sota, and S. Nakamura, Mater. Sci. Eng. B **59**, 298 (1999).
[24]T. T. Chen, C. L. Cheng, Y. F. Chen, F. Y. Chang, H. H. Lin, C.-T. Wu, and C.-H. Chen, Phys. Rev. B. **75**, 033310 (2007).
[25]S. D. Singh, V. K. Dixit, S. Porwal, R. Kumar, A. K. Srivastava, T. Ganguli, T. K. Sharma, and S. M. Oak, Appl. Phys. Lett. **97**, 111912 (2010).
[26]D. Alonso-Álvarez, B. Alén, J. M. Gercía, and J. M. Ripalda, Appl. Phys. Lett. **91**, 263103 (2007).
[27]Y.-H. Cho, G. H. Gainer, J. B. Lam, and J. J. Song, Phys. Rev. B. **61**, 7203 (2000).
[28]P. G. Eliseev, P. Perlin, J. Lee, and M. Osiński, Appl. Phys. Lett. **71**, 569 (1997).
[29]V. A. Fonoberov, K. A. Alim, A. A. Balandin, F. Xiu, and J. Liu, Phys. Rev. B. **73**, 165317 (2006).
[30]C. Gourdon and P. Lavallard, Phys. Status Solidi B **153**, 641 (1989).
[31]Y. Narukawa, Y. Kawakami, S. Fujita, and S. Fujita, Phys. Rev. B **55**, R1938 (1997).
[32]S. F. Chichibu, T. Onuma, M. Kubota, and A. Uedono, J. Appl. Phys. **99**, 093505 (2006).
[33]P. Corfdir, J. Ristic, P. Lefebvre, T. Zhu, D. Martin, A. Dussaigne, J. D. Ganiere, N. Grandjean, and B. Deveaud-Pledran, Appl. Phys. Lett. **94**, 201115 (2009).
[34]T. Schmidt, K. Lischka, and W. Zulehner, Phys. Rev. B **45**, 8989 (1992).
[35]M. Strassburg, M. Dworzak, H. Born, R. Heitz, A. Hoffmann, M. Barteis, K. Lischka, D. Schikora, and J. Christen, Appl. Phys. Lett. **80**, 473 (2002).
[36]I. A. Buyanova, J. P. Bergman, G. Pozina, W. M. Chen, S. Rawal, D. P. Norton, S. J. Pearton, A. Osinsky, and J. W. Dong, Appl. Phys. Lett. **90**, 261907 (2007).

This article is copyrighted as indicated in the article. Reuse of AIP content is subject to the terms at: http://scitation.aip.org/termsconditions. Downloaded to IP: 140.113.38.11 On: Thu, 25 Dec 2014 02:22:50